One Year of Conjunction Events of ERS-1 and ERS-2 with Objects of the USSPACECOM Catalog

H. Klinkrad

Mission Analysis Section, ESA/ESOC
Darmstadt, Germany

Abstract

The current (Feb.1997) population of the orbit catalog of the US Space Command (USSPACECOM) contains some 8200 objects of which more than 2300 can pose a collision risk to the ERS-1 and ERS-2 spacecraft of the European Space Agency, which operate in a tandem configuration on sun-synchronous, near circular orbits of mean altitude 781 km. For both spacecraft ESOC performs conjunction event predictions and collision risk assessments in weekly intervals, based on a given catalog population, and based on estimates of the orbit prediction accuracies of the underlying TLE orbit data sets. Results of more than one year of ERS-1 and ERS-2 conjunction event forecasts are summarised and reviewed statistically as well as deterministically in case of critical fly-bys. The statistical distribution of conjunction events is analysed, and the orbital characteristics and physical dimensions of potential impactor objects from the catalog are identified. A collision reference ellipsoid of extension 25 km x 10 km x 10 km in along-track, radial, and out-of-plane direction is used as threshold for qualifying conjunctions. Near-miss events are assessed for their risk potential. The underlying theory and the importance of a priori knowledge on orbit determination uncertainties is explained in detail. The collision between the Helios-1A subsatellite Cerise and an Ariane fragment is described to illustrate the risk potential in ERS similar orbits.

1. Introduction

As of February 1997 the catalog of USSPACECOM contains the orbits of 8,213 objects (not including so-called 'Analyst Sets'). This is the remaining on-orbit population resulting from more than 3,800 launches since 1957. In particular, more than 130 on orbit fragmentations of rocket upper stages and satellites since 1961 have contributed 55% to the trackable population. Another 20% of the catalog are defunct satellites, 16% are rocket upper stages, and only about 6% are operational payloads. The Space Surveillance System (SSN) of the US Space Command (USSPACECOM) is regularly tracking, correlating, and cataloging space objects of sizes larger than 10 cm in low earth orbit (LEO) and larger than 1 m in the geostationary orbit (GEO). Radar detectors are mainly surveilling the space up to 2,000 km altitude, while tracking data from electro-optical telescopes are prevailing beyond 2,000 km altitude up to GEO. Experimental radar and optical observation campaigns have demonstrated that at the lower end of the SSN detection threshold (for $10cm \leq d \leq 1m$) the derived catalog may be incomplete by a factor 2. Objects in the size class $0.3cm \leq d \leq 0.6cm$, which could still disable or destroy an unshielded spacecraft, are likely to outnumber the catalog by a factor of up to 100. Debris of diameters $d \geq 1cm$, which cannot be shielded with current on-orbit technologies, are estimated to be between 8 to 20 times more abundant than the trackable objects of the current catalog (yielding 65,000 to 150,000 objects).

As a consequence of the steady growth of space debris, the resulting collision risk which is imposed on large-size orbiting targets has in recent years become a non-negligible factor for launch and on-orbit operations. For Space Shuttle, USSPACECOM in cooperation with NASA are routinely performing collision-free launch window determinations (ORBWIN software, Ref.1), and computations of near-misses between Space Shuttle and members of the catalog population (COMBO software: Computation of Miss Between Orbits, Ref.8). The decision to monitor and forecast near-miss events of catalog objects with respect to Space Shuttle was taken after the Challenger STS-51L accident. Based on studies of orbit determination accuracies for Space Shuttle and for catalog objects, an STS operational flight rule was established (JSC-12820, Rule 4-61) which triggers collision avoidance procedures if the predicted miss distance is within a target centered manoeuvre ellipsoid of 5km x 2km x 2km (along-track, radial, out-of-plane), and if neither payload nor mission objectives are compromised (Ref.9). This collision ellipsoid corresponds to an accepted residual risk of 1 in 100,000. Once a catalog object is predicted to pass within a warning ellipsoid of 25km x 5km x 5km the tasking of SSN sensors is intensified to reduce orbit determination errors and thus improve the conjunction event prediction and the assessment of the associated risk. Statistical estimates indicate that for an STS mission of standard altitude, inclination, and mission duration about 1 avoidance manoeuvre can be expected every 10 missions. This forecast figure matches well with operational records: During the 49 Shuttle missions from STS-26 to STS-72 (exluding the STS-51L Challenger accident), there were 24 passes of objects within the alert ellipsoid, and 6 passes within the manoeuvre ellipsoid. For 3 of these avoidance manoeuvres were initiated (STS-48 on 17-Sep-91 to avoid the Kosmos-955 upper stage, STS-44

Proceedings of the Second European Conference on Space Debris, ESOC, Darmstadt, Germany, 17-19 March 1997, (ESA SP-393, May 1997)

on 29-Nov-91 to avoid the Kosmos-851 upper stage, and STS-53 on 08-Dec-92 to avoid a MIR debris).

In contrast with the Space Shuttle, which primarily operates on moderately inclined orbits between 400 and 600 km altitude, the European Remote Sensing satellites ERS-1 and ERS-2 perform their earth observation mission from high inclination, sun-synchronous orbits of mean altitudes of 781 km. The corresponding catalog object flux is at least 5 times larger than for the Shuttle. In order to assess the resulting collision risk for ERS-1 and ERS-2, the European Space Operations Centre (ESOC) is performing weekly conjunction event predictions for their spacecraft with objects from the most recent catalog. Results of these near-miss predictions during a time span of 14 months will be analysed in the following. As an illustration of the non-negligible risk on ERS-type orbits the collision of the Helios-1A subsatellite Cerise with an explosion fragment of the SPOT-1 upper stage will be reviewed.

2. Computation of Conjunction Events

2.1 The ERS-1 and ERS-2 Spacecraft

ERS-1 (91-050A) was launched from Kourou on an Ariane-1 on 21-Jul-1991 (see Fig.1 for an illustration of ERS-1). Four years later, on 21-Apr-1995, ERS-2 (95-021A) was launched from the same site on an Ariane-40. Both spacecraft perform remote sensing of the earth and ocean surface by means of a radar altimeter, a windscatterometer, a synthetic aperture radar, an along-track scanning radiometer, and a microwave sounder. Moreover, both spacecraft support high accuracy orbit determination for geodesy applications by means of laser retro-reflectors and a precise range and range-rate equipment (PRARE). Since 1995 both spacecraft have been operated in a tandem mode, where ERS-1 exactly follows the ERS-2 groundtrack with a delay of one day. Their groundtrack and orbit period is phased such that they revisit the same geographic location after 35 days and 501 orbits.

ERS-1 and ERS-2 are flying on near-circular, sun-synchronous orbits of mean altitude 781.1 km. The semimajor axis of $a = 7159.235$ km is kept within tight limits to guarantee a groundtrack offset of less that 1 km (necessitating about one Δa correction every 30 days and one Δi correction every 70 to 140 days). The sun-synchronous inclination for the ERS altitude is $i = 98.5227°$. The choice and maintenance of the eccentricity $e = 0.001165$ and argument of perigee $\omega = 90.0°$ allow to keep the spacecraft in a "frozen perigee" orbit with near-constant altitude profiles as a function of latitude. Operational orbit determination is performed using Kiruna S-band range and range-rate measurements, and global altimeter data which are downloaded at Kiruna. The rms accuracy of the resulting orbit fits is 2-4 m along-track, 1-2 m cross-track, and 0.5 m in radial direction.

2.2 Orbit Determination Uncertainties

In order to associate miss distances between any two catalog objects with a corresponding collision risk, one must have some knowledge of the uncertainty which is related to the predicted positions of the objects. The catalog two-line element sets (dubbed also TLEs or ELSETs) are received at ESOC from NASA's Goddard Space Flight Center (GSFC) every 2 to 3 days. Using a representative sample of 371 TLE data sets of ERS-1 over the time period 21-Jul-1991 to 26-Jan-1993, catalog orbit determination uncertainties could be derived by comparison with the ESOC orbit fits during periods with and without manoeuvres. The results are summarised in Tab.1 for manoeuvre free periods in terms of along-track, radial, and out-of-plane position and velocity errors, and in terms of corresponding rms uncertainties in the Kepler orbital elements. The rms errors of the TLE orbit determinations for ERS-1 can increase by a factor 2 in along-track, and a factor 3-4 in radial and out-of-plane direction during manoeuvre periods. A similar analysis was performed to assess the TLE errors for ESA's EURECA platform which was released by STS-46 on 02-Aug-1992 into a 450 km orbit at 28.5° inclination. The resulting 2 σ position uncertainty matches the 5km × 2km × 2km manoeuvre ellipsoid adopted for Shuttle operations.

The orbit determination accuracy assessment just described is based on interpolated ESOC states of well defined accuracy for epochs of TLE orbit determinations (at ascending nodes). Thus, TLE propagation errors were eliminated. The concurrent states were then transformed to osculating cartesian state vectors in a true-of-date equatorial system using the SGP-4 orbit theory for the TLE transformations. Error contributions from ERS-1 reference orbit determinations performed by ESOC to the overall rms uncertainties and maximum offsets listed in Tab.1 can be neglected, since they are about 2 orders of magnitude smaller.

2.3 Prediction of Conjunction Events

In the following conjunction events of objects from the USSPACECOM catalog population with respect to the ERS-1 and ERS-2 satellites shall be analysed. A conjunction event shall be defined as a fly-by of a catalog object at a closest distance which lies inside a "reference ellipsoid" $d_u \times d_v \times d_w$ of dimensions 10km × 25km × 10km in the radial, along-track, and out-of-plane direction of a spacecraft centered coordinate system (this corresponds to the Shuttle manoeuvre ellipsoid enlarged by a factor 5).

The conjunction event detection algorithm which is used by ESOC is closely following the processing steps outlined in Ref.3. The following successive sieves are used to determine potential near-miss or collision events:

- Epoch Filter: rejection of all TLE states which have an epoch which is more than Δt_{TLE} days before the reference epoch (e.g. $\Delta t_{TLE} \geq \Delta t_{max} = 30$d), in order to discard unreliable data sets.

- Altitude Filter: rejection of all TLE states which, when considering altitude decay, do not intersect the altitude band defined by the initial apogee and final perigee of the target orbit within the analysis time span.

- Plane & Geometry Filter: rejection of all TLE orbits which at the intersection of the chaser and target orbit plane have position separations larger than the maximum extension of the collision reference ellipsoid ($\Delta r_{min} \geq \Delta d_v$).

- Orbit Phase Filter: rejection of those TLE orbits which at times of possible conjunctions do not yield

orbit positions within the collision reference ellipsoid $d_u \times d_v \times d_w$ of the target spacecraft.

The acceptance of a conjunction event by the orbit phase filter is controlled by the magnitude of k in the following definition of a target centered ellipsoid.

$$k^2 = \frac{\Delta r_u^2}{d_u^2} + \frac{\Delta r_v^2}{d_v^2} + \frac{\Delta r_w^2}{d_w^2} \qquad (1)$$

For $k^2 < 1$ the closest fly-by distance is inside the collision reference ellipsoid. In this case the quantity $f(k) = 1/k$ indicates within what fraction of the reference ellipsoid the fly-by occurs (assuming that a common scaling factor is applied to the main axes).

The fly-by distance $\Delta\underline{r} = \underline{r}_c - \underline{r}_t$ (where c stands for chaser, and t stands for target) can be described in the target centered orbit coordinate system $\underline{u}$, $\underline{v}$, and $\underline{w}$ (in radial, along-track, and out-of-plane direction) by forming the scalar products with these unit vectors to obtain Δr_u, Δr_v,and Δr_w. The fly-by distance Δr, the azimuth angle A, and elevation angle h of the conjunction direction (see Fig.1) are then defined as

$$\Delta r = \sqrt{\Delta r_u^2 + \Delta r_v^2 + \Delta r_w^2} \qquad (2)$$

$$A = 2 \operatorname{arctg}\left(\frac{\Delta r_v - \sqrt{\Delta r_v^2 + \Delta r_w^2}}{\Delta r_w} \right) \qquad (3)$$

$$h = \arcsin(\Delta r_u / \Delta r) \qquad (4)$$

where A is measured in the local horizontal plane, in a clock-wise sense, starting from the target's flight direction, and h is counted from the horizontal plane, positive towards space.

The time of closest approach t_{con} is determined by iteratively solving for a zero transition of the range-rate $\dot{\rho}(t)$ between target and chaser.

$$\dot{\rho}(t_{con}) = 0 = (\dot{\underline{r}}_c(t_{con}) - \dot{\underline{r}}_t(t_{con})) \bullet \Delta\underline{r}(t_{con}) \qquad (5)$$

At the conjunction event time t_{con} the relative velocity of the chaser with respect to the center of the moving target is defined as $\Delta\underline{V} = \Delta\dot{\underline{r}} = \dot{\underline{r}}_c - \dot{\underline{r}}_t$. This would be the collision velocity in case of a direct hit. The azimuth and elevation angles of the relative velocity in the target centered system can be dereived as before by means of eq.(3) and (4).

2.4 Assessment of Collision Probability

The distance $\Delta r(t_{con})$ of a conjunction event does not necessarily reflect the associated risk. The parameter k in eq.(1) is better suited since it roughly accounts for the position uncertainties of the target, but it still does not include orbit errors of the chaser object, nor does it consider the change of the position error ellipsoids of the target and the chaser with increasing time separation from the TLE orbit determination epoch. The following theory has been devised to overcome such deficiencies and yield a tangible and reliable number for the collision probability associated with a conjunction event.

When assessing ERS-1 and ERS-2 conjunction events with catalog objects it shall be assumed that both ERS spacecraft have TLE orbit determination errors corresponding to the 1σ Kepler element uncertainties listed in Tab.1, and that ballistic parameter information (i.e. the TLE quantity $\dot{n}/2$) has a 1σ uncertainty corresponding to 10% of its magnitude. For the chaser objects a 20% larger rms error shall be adopted for the same parameter set.

Let the state parameters $\underline{x} = (x_1, \ldots, x_n)$ at TLE orbit determination epoch t_{tle} have 1σ uncertainties of $\underline{\sigma}_x = (\sigma_{x,1}, \ldots, \sigma_{x,n})$, corresponding to $\sigma_{x,1} = \Delta a_{1\sigma}$, $\sigma_{x,2} = \Delta e_{1\sigma}$, $\sigma_{x,3} = \Delta i_{1\sigma}$, $\sigma_{x,4} = \Delta\Omega_{1\sigma}$, $\sigma_{x,5} = \Delta u_{1\sigma}$ (where $u = \omega + f$), and $\sigma_{x,6} = \Delta\dot{n}_{1\sigma}$. The diagonal elements of the initial error covariance matrix $E(t_{tle})$ can then be assigned to $E_{i,i} = \sigma_{x,1}^2, \ldots, \sigma_{x,6}^2$ for $i = 1, \ldots, n$. The effect of these initial uncertainties on the predicted orbit position at the time of conjunction t_{con} can be expressed by a transition matrix Φ.

$$\Phi_{j,i}(t_{tle}, t_{con}) = \frac{d(\Delta r_u(t_{con}))}{dx_i(t_{tle})} \qquad u \rightarrow v, w \qquad (6)$$

where $j = 1, \ldots, m$ (with $m = 3$) corresponds to the u, v, w components of the position offset in the orbit coordinate system of the nominal state prediction. The 3×6 matrix Φ is generated by finite differences, using a comprehensive orbit propagation theory including the zonals J_2 to J_5 and atmospheric drag. The transition matrix $\Phi(t_{tle},t_{con})$ can be used to map the initial state parameter variances $E(t_{tle})$ onto position uncertainties at the fly-by epoch t_{con}.

$$F(t_{con}) = \Phi(t_{tle}, t_{con})\, E(t_{tle})\, \Phi^T(t_{tle}, t_{con}) \qquad (7)$$

where $F(t_{con})$ is the 3×3 error covariance matrix of the orbit position at the conjunction epoch. The 3 eigenvalues λ_j of $F(t_{con})$ define the length of the main axes $b_j = \sqrt{\lambda_j}$ of the 1σ position error ellipsoid, while the corresponding eigenvectors $\underline{e}_j = (e_{j,u}, e_{j,v}, e_{j,w})$ indicate the orientation of the axes in the spacecraft centered $\underline{u}$, $\underline{v}$, $\underline{w}$ coordinate system. Their directional angles can be determined via eq.(3) and (4).

The 3 dimensional position probability density function of an object, based on normally distributed errors of initial parameters, is defined as

$$p(\Delta\underline{r}) = \frac{1}{\sqrt{(2\pi)^3 \operatorname{Det}(F)}} \exp\left[-\frac{1}{2} \Delta\underline{r}^T F^{-1} \Delta\underline{r} \right] \qquad (8)$$

This function describes the resident probability per unit volume at a location with an offset of $\Delta\underline{r}(t_{con})$ from the nominally predicted object position $\underline{r}(t_{con})$ at the time of a conjunction event. The highest probability density p_{max} is obtained at the nominal position where $\Delta\underline{r} = \underline{0}$.

$$p_{max} = \frac{1}{\sqrt{(2\pi)^3 \operatorname{Det}(F)}} \qquad (9)$$

The probability $P_{t \rightarrow c}$ that a target object (index t) on its nominal orbit is colliding with a chaser object (index c) on an error affected orbit can be described as the volume integral with respect to the chaser's probability density $p_c(\Delta\underline{r})$, along the relative flight path $\Delta\underline{r}_t$ of the target which sweeps out a cylindrical volume of collision cross-section A_{col} (with A_{col} defined by the dimensions of the target and the chaser).

$$P_{t \rightarrow c} = \int_{\Delta t_{con} = -\infty}^{+\infty} p_c(\Delta\underline{r}_t(\Delta t_{con})) \, | \Delta\dot{\underline{r}}_t(t_{con}) | \, A_{col} \, dt \qquad (10)$$

$$\Delta\underline{r}_t(\Delta t_{con}) = \Delta\underline{r}_t(t_{con}) + \Delta t_{con} \, \Delta\dot{\underline{r}}_t(t_{con}) \qquad (11)$$

where $\Delta t_{con} = t - t_{con}$, and $|\Delta \dot{\underline{r}}_t(t_{con})| = \Delta V_t$ is the relative approach velocity in case of a direct hit. For software implementation purposes, the integral of eq.(10) can be approximated by a summation over a finite length of the relative flight path of the target. The increment of the timesteps Δt can be adjusted according to the value of p_{max}, and depending on the orientation of the flight path with respect to the main axes of the error ellipsoid. The summation limits can be chosen according to a selected threshold value for the $\Delta P_{t \to c}$ contributions.

The determination of the collision probability $P_{c \to t}$ of a nominal target orbit and an error affected chaser orbit is performed similarly as for $P_{t \to c}$. The total collision risk for a single conjunction event can then be described as the conditional probability

$$P_{col} = P_{c \to t} + P_{t \to c} - P_{c \to t} P_{t \to c} \qquad (12)$$

with each individual probability P_{col}, $P_{c \to t}$, and $P_{t \to c}$ constrained to $0 \leq P \leq 1$. The following risk assessments are based on this procedure, assuming a constant collision cross-section for ERS-1/ERS-2 and catalog objects of $A_{col} = 100\ m^2$, and assuming initial TLE orbit determination uncertainties based on the calibration results in Tab.1 .

3. Discussion of Results

3.1 Pre-Processing of TLE Data Sets

By screening the USSPACECOM catalog population of 8210 on 17-Feb-1997, 382 objects (4.6%) were rejected since they were in their final orbit decay, or since their orbit determination epoch was more than 30 days old (mostly for HEO and GEO type orbits). Based on the ERS-1/ERS-2 target orbits, the altitude filter removed another 5457 objects (66.5%), and the orbit plane filter rejected 53 further objects (0.6%). Subsequently, 2318 orbits were submitted to the orbit phase filter for a one week analysis time span. 60 TLE data sets for ERS-1, and 70 data sets for ERS-2 (about 1.5%) passed this filter and yielded 69 and 78 conjunction events, respectively, within a target centered reference ellipsoid of 25km x 10km x 10km. Of the 7828 TLE orbits analysed, only 456 (5.8%) had orbit determination dates which were more than 5 days before the reference epoch 17-Feb-1997 00:00 UT. The majority of data (70%) were less than 2 days old.

3.2 ERS-1 and ERS-2 Conjunction Events

In the adopted analysis time frame, between 04-Dec-1995 and 17-Feb-1997, conjunction events of ERS-1 and ERS-2 with objects of the USSPACECOM catalog were determined on a weekly basis, using the Monday catalog to predict fly-bys for the subsequent 7 days. In a first step, conjunction events were determined deterministically, assuming that the TLE data and the propagation method introduce no errors. Tab.1 shows that in total 4596 conjunctions met the proximity criterion of eq.(1) for a reference collision ellipsoid of 25km x 10km x 10km in along-track, radial, and out-of-plane direction of the nominal target position. 1167 passes occurred with 1/2 of this ellipsoid, 189 were within 1/5 (which is the Shuttle manoeuvre ellipsoid), 44 were within 1/10, and 8 events had miss distances within 1/20 (1.25km x 0.5km x 0.5km) of the original threshold volume. If Shuttle operations criteria would be applied, ERS-1 would have had 103, and ERS-2 would have had 86 evasive manoeuvres executed within 14 months. The closest predicted fly-bys (both of them for ERS-1) were recorded at distances within less than 1/40 of the reference ellipsoid (625m× 250m x 250m). Due to the high inclination of the ERS target orbits, most of the conjunction events were recorded at the extrema of the latitude band $\phi \in [-81.5°, +81.5°]$ which are prescribed by $i_{ERS} = 98.52°$ (see Fig.4). Local peaks at $\phi = \pm 74°$ are due to the dominance of the related inclination band which accounts for 50% of all potential colliders. Since the 74° inclinations are primarily occupied by Russian objects, Russia also dominates the ERS conjunction statistics with 59% of all events (USA: 31%, others: 10%). Of the 4596 registered fly-bys, 49% were with explosion fragments, 28% were with operational and non-operational payloads, and 23% were with rocket upper stages.

The orbits of those catalog objects which cause conjunction events with ERS-1 and ERS-2 are mostly near-circular, with semimajor axes in close neighbourhood of the target orbits. 54% of all conjunction orbits of chaser objects have semimajor axes with offsets $\Delta a \leq \pm 10$ km relative to the target orbits. Only 4% of the Δa's are outside a $\pm$ 150 km bandwidth. The statistical distribution of inclinations of potential collision partners is less uniform: 95% of all chaser orbits have inclinations of $65° \leq i_c \leq 100°$, with almost 50% of these resulting from the norrow inclination band $74.0° \leq i_c \leq 74.5°$. About 30% of the conjunction events can be attributed to sun-synchronous orbits of $97.5° \leq i_c \leq 100.5°$, and the remaining 20% are related to population clusters at $i_c = 66°, 71°, 82°$, and 90°.

The dominance of near-circular chaser orbits near the ERS-1 and ERS-2 altitudes and at 74° inclination is also evident from the summary of frequent revisits by the same chasers in Tab.3. ERS-1 had more that 20 conjunction events within 14 months with 7 catalog objects. For object 84-019B (the Kosmos-1538 SL-8 upper stage of 7.4 m length, 2.4 m diameter, and 2200 kg mass), 47 conjunctions were recorded in 3 distinct groups of which 41 events can be attributed to a single 2.8 day period, starting in 18-Jul-1996 at 04:37:30 UT, with a closest approach of 787 m. The other ERS-1 re-visitors were 4 more SL-8 upper stages (83-031B, 74-071B, 76-098B, and 86-030B), and 2 Kosmos satellites (72-104A and 72-043A, of about 750 kg each). In spite of the frequent conjunctions, the fly-by geometries of these ERS-1 passes did not qualify them as high risk events. In case of ERS-2 only 3 frequent re-visitors had more than 20 conjunction events during the analysed time span. For object 90-005H (the SPOT-2 Ariane-4 upper stage of 9.9 m length, 2.6 m diameter, and 1270 kg mass), however, 69 conjunctions were detected in a single 4.1 d period starting 11-Oct-1996 at 03:02:09 UT. The closest pass was at 4.45 km. The other re-visitors, 82-051E and 71-120C (debris from a SL-3 and a SL-8 upper stage, respectively), yielded more critical miss distances at 1.3 km and 280 m. The object 71-120C also caused the highest collision probability within the 14 months period of analysis (see Tab.4).

ERS-1 was launched with 4 other satellites: UOSAT-5 (91-050B), OrbComm-X (91-050C), TUBSAT-1 (91-050D), and SARA (91-050E). Of these, only UOSAT-5 had a conjunction with ERS-1, and TUBSAT-1 had a fly-by with ERS-2, both more than 10 km away. The Ariane 1 upper

stage (91-050F) of ERS-1, however, was passing ERS-1 within less than 15 km at 6 occasions (nearest miss distance: 7.3 km), and it had 1 conjunction with ERS-2. The ERS-2 Ariane 40 upper stage (95-021B) passed through the 25km × 10km × 10km reference ellipsoid of ERS-1 at 9 occasions (closest fly-by: 8.7 km), while there were 4 such events for ERS-2 with even closer proximities (at distances between 7.5 km and 3.7 km).

3.3 ERS-1 and ERS-2 Collision Risk

A synthesis of all conjunction events with a collision probability larger than 1 in 1,000,000 ($P_{col} \geq 10^{-6}$) is given in Tab.4 for ERS-1 and ERS-2 individually. The table indicates epoch and fly-by geometry of a conjunction event together with the associated collision probability and the impact velocity in case of a direct hit. The final columns give an indication on the reliability of the prediction by listing the propagation time span for the target and the chaser from the latest TLE orbit determination to the fly-by epoch. These time spans also govern the spread of the probability density functions in eq.(8) which determine the collision risk for a particular event.

The number of the extracted high risk conjunctions (see Tab.1) is balanced between ERS-1 and ERS-2, with 7 near-misses each of a collision probability $P_{col} \geq 10^{-6}$. Due to the tube-like along-track extension of the target centered position error ellipsoid, and due to the rapid drop-off of the resulting probability densities in radial and out-of-plane direction, the highest collision risk can be expected for aligned velocity vectors of the target and the chaser. This is probable in case of co-planar trajectories and co- or counter-rotating orbits. For the ERS satellites, co-rotation with possible "resonant" conjunctions over extended periods of time can occur for chaser inclinations near $i_c = 98.52°$ (see 90-005H in Tab.3). High risk conjunctions for counter-rotating orbits are likely to occur for chaser inclinations around $i_c = 81.48°$, which is the complementary ERS inclination ($i_c = 180° - i_{ERS}$). These orbits (see 71-120C in Tab.3) yield the highest possible relative collision velocities of about 15 km/s.

Over the analysis time span from 04-Dec-1995 to 17-Feb-1997 the most critical fly-by was recorded for object 71-120C (an SL-3 upper stage debris of the Meteor-10 launch) with respect to ERS-2, on 05-Feb-1996 15:15:01 UT, at a distance of 670m (see Tab.4). The closest approach was near the local horizontal plane (elevation $h = 8.6°$), almost perpendicular to the satellite flight path (azimuth $A = -90.56°$). In this scenario the collision velocity vector is almost aligned with the ERS-2 trajectory ($A = 179.4°$), reaching a ΔV of 14.9 km/s, close to the theoretical maximum. The chaser object can hence sweep out a large volume of the target's probability density function (position error ellipsoid) with an assumed collision cross-section of $A_{col} = 100\ m^2$. Based on the procedures described in chapter 2.4, the ERS-2/71-120C collision probability is estimated to be 1.11×10^{-4}, or 1 :9009 (Fig.2 illustrates the near-miss scenario). Two days before this event, on 05-Feb-1996 07:51:14 UT, the same two objects had a conjunction at a distance of 434m. Since this pass was below the horizontal plane ($h = -42.7°$), the resulting collision risk was only 7.5×10^{-5}, or 1 :13300. Almost the same risk level was determined for the worst case ERS-1 conjunction event with object 81-041B (an SL-8 upper stage of 7.4m length, 2.4m diameter, and 2200 kg mass). The fly-by on 14-Mar-1996 at 02:17:18 UT was almost in the horizontal plane at a range of 750m, with a misalignment of the velocity vectors by $\Delta A = 12°$. All other conjunction events of ERS-1 were with explosion fragments or with upper stage debris. ERS-2, however, had some further fly-bys of massive spacecraft (74-063A: DMSP-6, 85-079A: Kosmos-1680, 76-069A: Kosmos-841). The overall statistics of relative velocities and their alignments with the target orbit is shown in Fig.6 and 7 for conjunction events of ERS-1 and ERS-2 within 1/2 and within 1/5 of the reference collision ellipsoid. Clearly, the most likely collision velocity is on the order of 15 km/s, and the most likely approach direction in case of a direct hit is along the flight path of the target orbit.

The results discussed so far are based on probability theory, and they produce finite probabilities of a collision for any conjunction event. While the individual risk for a single spacecraft may be low (for ERS-1 and ERS-2, the joint probability of collision with a catalog object is about 1:2000 per year), one must bear in mind that about 2300 trackable objects could collide with ERS-1 or ERS-2, or with each other. The 1:2000 annual risk for ERS-1/ERS-2 is based on an assumed collision cross-section of 100 m², which is too high when looking at collisions between objects at the lower size threshold of the catalog. If a collision cross-section of 3 m² is adopted instead (corresponding to 2 objects of 1 m diameter each), then the annual risk for an ERS-type orbit to have a collision with another catalog object will be on the order of 1:60, or one collision in every 60 years. This number agrees well with long-term predictions of space debris environment models. In spite of this long-term prospect, it seems that after 40 years of spaceflight such a collision between two catalog objects, the first one ever recorded, has occurred. On 24-Jul-1996 at 09:48:03 UT the French satellite Cerise (95-033B, lauched with Helios-1A) was hit by an explosion fragment (86-019RF) of the Ariane 1 upper stage which deployed SPOT-1. The two objects collided at $\phi = 38.18°S$ and $\lambda = 59.74°E$ in an altitude of 685.8 km, half way between Madagaskar and the Kerguelen islands (the Fig.3). A TLE based re-calculation of the conjunction event and a loss of the spacecraft attitude could be time correlated to within ± 2.5 sec, and provided strong evidence of a collision. Further proof was provided by the German FGAN radar which shortly after the event observed the tumbling Cerise spacecraft, and a part of the gravity gradient boom of about 4m length (including the end mass). It appears that the boom was severed during the collision at a distance of about 2m from the satellite body.

4. Summary and Conclusions

For an ERS-1 or ERS-2 type near circular orbit of a sun-synchronous inclination of 98.52° and a mean altitude of 781 km, the probability to collide with one of the 8210 objects of the USSPACECOM catalog of 17-Feb-1997 is on the order of 1 : 400,000 for each m² of collision cross-section and year of operation. This result, which is based on the analysis of 14 months of conjunction event predictions (from 04-Dec-1995 to 17-Feb-1997), is on the same order of magnitude as a statistical prediction of the collision flux with catalog objects of sizes $d > 10$ cm (the SSN detection threshold) for the same orbit. ESA's MASTER debris model estimates this catalog object flux to be $8.7 \times 10^{-6}\ m^{-2}\ yr^{-1}$

(Ref.6), corresponding to an annual collision probability per m^2 of cross-section of 1 :116,000. The latter number includes the so-called "Henize Factor" of about 2.0 to account for the incompleteness of the catalog at its lower size threshold. When the same correction is applied to the conjunction based, deterministic collision probability, then the agreement with the MASTER result is within 70%, which gives confidence in the adequacy of the sampling period and in the algorithms of the conjunction event analysis. The mean time between collisions of an ERS-type orbit and a catalog object, based on 14 months of ERS conjunction events, is estimated to be 60 years (assuming diameters of 1 m for both objects). This number is again in good agreement with long-term debris environment prediction models (Ref.6).

In order to reduce the collision risk associated with a predicted conjunction of ERS-1 or ERS-2 with catalog objects, one could execute an avoidance manoeuvre if a certain threshold probability is exceeded. The necessary ΔV's are normally less than 1 m/s, and they change semimajor axis and eccentricity such that a sufficient vertical separation at the time of conjunction is acquired (this is the direction in which the position error ellipsoid has its smallest extension). For the ERS satellites such procedures are not yet in place. For the Space Shuttle, however, evasive manoeuvres are executed if a conjunction event is predicted to occur within an ellipsoid of extension 5km x 2km x 2km (along-track, radial, out-of-plane), and if neither payload nor mission objectives are compromised. This was the case at 3 occasions so far (STS-48, STS-44, and STS-53). For the ERS spacecraft, an application of the same flight rule would have resulted in about 80 avoidance manoeuvres per spacecraft and year of operation, which would severely degrade the quality of ERS mission products, and cause excessive operational work load. Consequently, an operationally feasible collision avoidance policy for ERS-1 and ERS-2 must accept collision probabilities which are on the order of 1:10,000 or 1:20,000, and which are hence by a factor 5 to 10 higher than for the Space Shuttle.

Acknowledgements

The assistance of Cristina Hernandez, GVM S.A., in the processing of the conjunction statistics is gratefully acknowledged.

References

1. G.D.Bredvik, J.E.Strub
Determination of Acceptable Launch Windows for Satellite Collision Avoidance
Paper **AAS 91-373**, AAS/AIAA Astrodynamics Specialist Conference, Durango/CO, Aug.19-22, 1991

2. K.J.Ernandes
A Mission-Preserving Evasion Technique for Near-Circular, Low-Altitude Orbits
Paper **AIAA 88-4278-CP**, 1988

3. F.R.Hoots, L.L.Crawford, R.L.Roehrich
An Analytical Method to Determine Future Close Approaches Between Satellites
Celestial Mech. 33 (1984), p.143-158

4. E.L. Jenkins, P.W. Schumacher
Predicting Conjunctions with Trackable Space Debris: Some Recent Experiences
Paper **AAS-97-014**, 20th Annual AAS Guidance and Control Conference, Breckenridge/Co., Feb.5-9, 1997

5. H. Klinkrad
Analysis of Near-Misses Between Operational Spacecraft and Catalog Objects
ESA SD-01, Proceedings of the First European Conference on Space Debris, Darmstadt, Germany, 5-7 April, 1993

6. H. Klinkrad
Description and Forecast of the Terrestrial Space Debris Environment
ESA Conference on Spacecraft Structures, Materials, and Testing, Noordwijk, The Netherlands, 27-29 March, 1996

7. J.J.F.Liu, R.L.Alford
A Semi-Analytic Theory for the Motion of a Close-Earth Artificial Satellite with Drag
Paper **AIAA 79-0123**, 17th Aerospace Sciences Meeting, New Orleans/La., Jan.15-17, 1979

8. J.P.Loftus, P.Anz-Meador, R.Reynolds
Orbital Debris Mitigation Techniques
Adv. Space Res., Vol.13, No.8, pp. 263-282, 1993

9. F.Vilas, M.Collins, P.Kramer, G.Arndt, J.Suddath
Collision Warning and Avoidance Considerations for the Space Shuttle and Space Station Freedom
Paper **AIAA 90-1337**, AIAA/NASA/DOD Orbital Debris Conference, Baltimore/MD, Apr.16-19, 1990

ERS-1 TLE Position Errors (km)						ERS-1 TLE Velocity Errors (m/s)					
along-track		radial		out-of-plane		along-track		radial		out-of-plane	
RMS	Max	RMS	Max	RMS	Max	RMS	Max	RMS	Max	RMS	Max
2.318	11.801	0.212	0.775	0.226	0.784	0.220	0.800	2.437	12.576	0.488	2.903

ERS-1 TLE Kepler Element Errors											
Δa(m)		$\Delta e \times 10^3$		$\Delta i(°) \times 10^3$		$\Delta\Omega(°) \times 10^3$		$\Delta\omega(°)$		$\Delta f(°)$	
RMS	Max	RMS	Max	RMS	Max	RMS	Max	RMS	Max	RMS	Max
57.184	198.61	0.027	0.097	3.748	22.299	1.831	6.327	1.487	5.223	1.486	5.212

Tab.1: Assessment of TLE orbit determination accuracies for ERS-1 (91-050A) for an analysis period between 21-Jul-91 and 26-Jan-93 (comprising 371 TLE orbit states). Interpolated ESOC precise orbit determinations were used as references (related RMS position uncertainties along-track, radial, and out-of-plane: 10m × 1m × 2m).

Conjunction Events within Fractions of an Adopted ERS Collision Reference Ellipsoid of 25 km × 10 km × 10 km (along-track × radial × out-of-plane)								
Fraction of Ref. Ellipsoid	1/1	1/2	1/3	1/5	1/10	1/15	1/20	< 1/25
ERS-1 Conjunctions	2323	600	282	103	22	12	7	5
ERS-2 Conjunctions	2273	567	231	86	22	6	1	1
Total Conjunctions	4596	1167	513	189	44	18	8	6

Tab.2: Conjunction events of the ERS-1 and ERS-2 satellites with members of the USSPACECOM catalog population as function of the fly-by distance expressed in fractions of a reference ellipsoid of extension 25 km × 10 km × 10 km (along-track × radial × out-of-plane). - The statistics relates to a period from 04-Dec-1995 to 17-Feb-1997.

Consecutive Conjunction Events of ERS-1 (91-050A) with Catalog Objects (04-Dec-1995 to 17-Feb-1997)										
Catalog Obj. ID	Total Fly-Bys		Longest Consecutive Group of Fly-Bys					Orbit of Catalog Object		
	Events	Groups	Events	Δt(d)	Begin of Fly-Bys within 25km × 10km × 10km		min. Δr(km)	a (km)	e (-)	i (°)
84-019B	47	3	41	2.793	96-Jul-18	04:37:29.94	0.787	7158.64	0.00305	74.041
72-104A	33	7	25	2.513	96-Sep-20	00:03:27.14	1.884	7154.74	0.00193	74.077
72-043A	31	7	21	1.397	96-Feb-05	11:22:09.87	4.018	7157.06	0.00042	74.052
76-098B	28	5	13	0.454	96-Jan-04	04:34:23.13	6.793	7153.28	0.00229	74.050
83-031B	26	6	8	0.384	96-Oct-16	15:52:00.59	1.817	7157.96	0.00078	74.050
74-071B	21	6	7	0.314	96-Apr-01	11:01:38.87	2.489	7157.36	0.00222	74.045
86-030B	21	4	9	0.454	96-Apr-04	07:47:58.81	3.871	7158.70	0.00216	74.024

Consecutive Conjunction Events of ERS-2 (95-021A) with Catalog Objects (04-Dec-1995 to 17-Feb-1997)										
Catalog Obj. ID	Total Fly-Bys		Longest Consecutive Group of Fly-Bys					Orbit of Catalog Object		
	Events	Groups	Events	Δt(d)	Begin of Fly-Bys within 25km × 10km × 10km		min. Δr(km)	a (km)	e (-)	i (°)
90-005H	69	1	69	4.087	96-Oct-11	03:02:09.11	4.451	7159.64	0.00196	98.351
82-051E	34	9	20	1.325	96-Oct-04	00:11:09.49	2.325	7149.72	0.00064	74.010
71-120C	30	12	5	0.280	96-Feb-03	04:29:51.74	0.434	7170.12	0.00180	81.238

Tab.3: List of catalog objects with more than 20 fly-bys of ERS-1 and ERS-2 within a target centered reference ellipsoid of extension 25km × 10km × 10km (along-track, radial, out-of-plane). Analysis timespan: 04-Dec-1995 to 17-Feb-1997.

Conjunction Events of ERS-1 (91-050A) with Catalog Objects (time span: 04-Dec-1995 to 17-Feb-1997)										
Catalog Obj. ID	Fly-By Epoch t_{ref} (UTC)		Fly-By Geometry			Collision Risk			Δt(d) = t_{TLE}-t_{ref}	
	yy-mmm-dd	hh:mm:ss.s	Δr(km)	Azi(°)	Ele(°)	Prob.	V(km/s)	Azi(°)	Δt_{ERS}	Δt_{obj}
81-041B	96-Mar-14	02:17:18.35	0.750	-78.00	0.63	7.85e-5	14.570	-168.00	-1.761	-1.979
65-020FF	96-May-17	16:52:25.43	0.245	73.14	-63.33	6.33e-6	14.268	161.17	-4.933	-4.536
92-093HL	96-Nov-11	17:56:39.45	0.603	-65.49	53.58	4.93e-6	13.666	-155.88	+0.824	+0.124
75-004HN	97-Jan-21	00:46:21.55	0.535	-45.08	48.79	4.85e-6	13.666	-155.88	+0.190	-5.618
87-098D	96-Jun-01	02:19:02.34	0.330	83.46	-62.05	4.37e-6	14.800	173.34	-4.936	-4.954
75-027C	96-Oct-17	13:42:21.55	0.895	35.90	-13.07	3.80e-6	8.733	125.95	-3.480	-3.645
78-026ET	96-Apr-30	07:40:02.40	0.399	-124.76	61.52	2.92e-6	12.130	144.49	-1.103	-1.460

Conjunction Events of ERS-2 (95-021A) with Catalog Objects (time span: 04-Dec-1995 to 17-Feb-1997)										
Catalog Obj. ID	Fly-By Epoch t_{ref} (UTC)		Fly-By Geometry			Collision Risk			Δt(d) = t_{TLE}-t_{ref}	
	yy-mmm-dd	hh:mm:ss.s	Δr(km)	Azi(°)	Ele(°)	Prob.	V(km/s)	Azi(°)	Δt_{ERS}	Δt_{obj}
71-120C	96-Feb-05	15:15:00.99	0.670	-90.56	8.57	1.11e-4	14.931	179.44	-0.509	-0.506
71-120C	96-Feb-03	07:51:14.69	0.434	91.69	-42.73	7.52e-5	14.924	-178.28	-1.134	-1.138
74-063A	96-Feb-28	23:57:59.35	1.077	119.80	-3.44	2.95e-5	12.932	-150.20	-0.748	-0.970
85-079A	96-Nov-27	11:05:38.10	0.442	-82.10	69.64	7.76e-6	14.752	-171.95	-0.268	-1.306
71-120C	95-Dec-06	12:54:16.01	0.869	30.94	20.48	6.16e-6	7.648	120.93	-0.399	-0.470
86-030C	96-Oct-11	03:56:28.47	0.664	131.00	-23.76	1.39e-6	11.245	-139.03	-4.037	-4.602
76-069A	96-Oct-10	04:43:20.88	19.499	166.97	0.86	1.11e-6	7.648	120.93	-1.044	-1.462

Tab.4: Summary of near-miss events of ERS-1 and ERS-2 with USSPACECOM catalog objects (sorted by risk level). Only those events are listed which result in a collision risk larger than $10^{-6} = 1 : 1{,}000{,}000$ within an analysis timespan between 04-Dec-1995 and 17-Feb-1997.

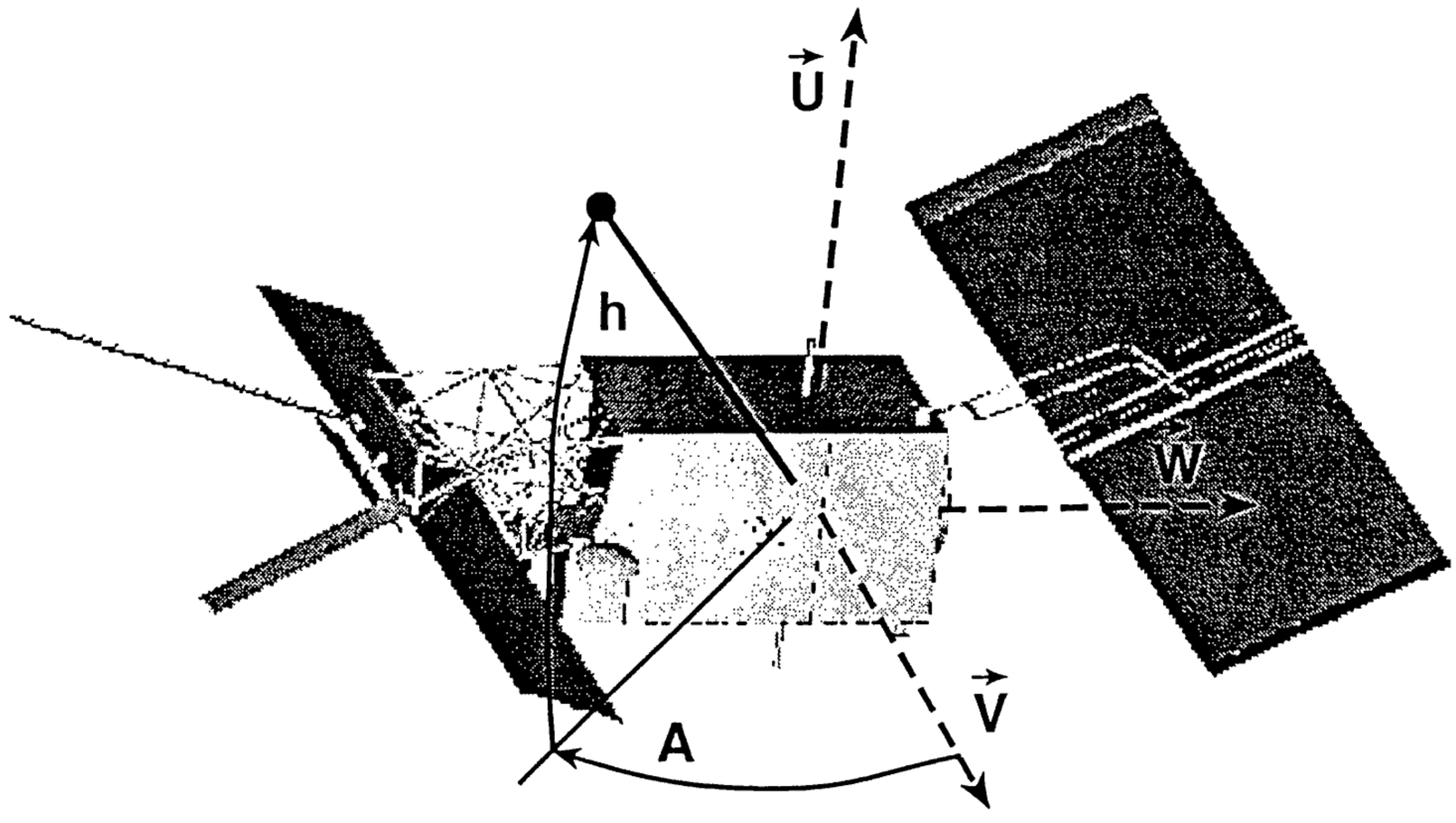

Fig.1: Definition of azimuth *A* and elevation *h* in a spacecraft centered U, V, W system (radial, along-track, out-of-plane) for a nominal flight attitude of ERS-1/ERS-2.

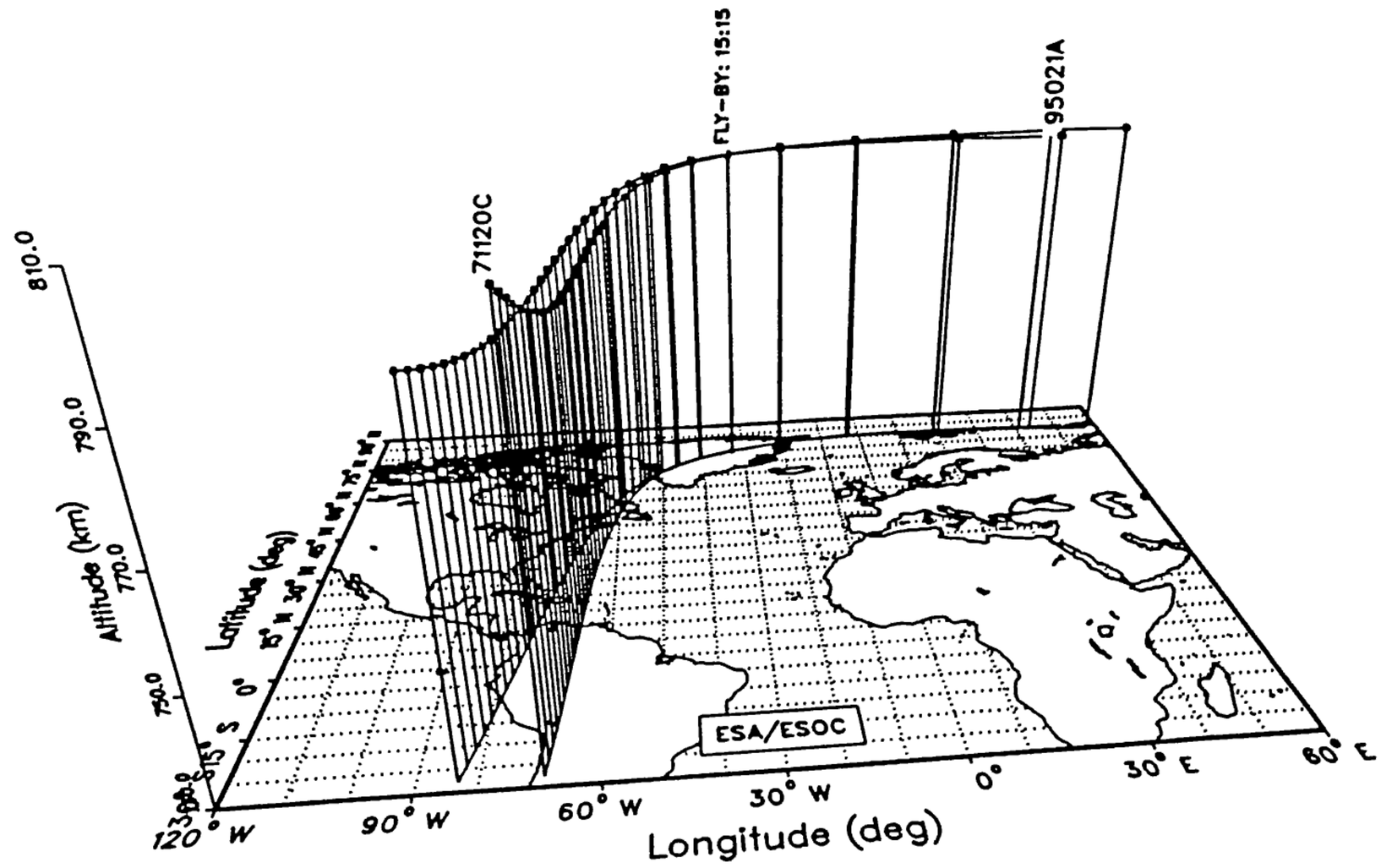

Fig.2: Near-miss of ERS-2 (95-021A) and a Meteor-10 rocket body debris (71-120C) on 05-Feb-1996 15:15:01 UT at $H = 796.14$ km, $\phi = 76.50°$ N and $\lambda = 32.64°$ W. The predicted fly-by distance of 670 m corresponds to a collision risk of 1 : 9009 for the closely aligned velocity vectors of opposite direction. - The COSPAR numbers indicate the start of the satellite tracks. Track markers are spaced at 1 min intervals.

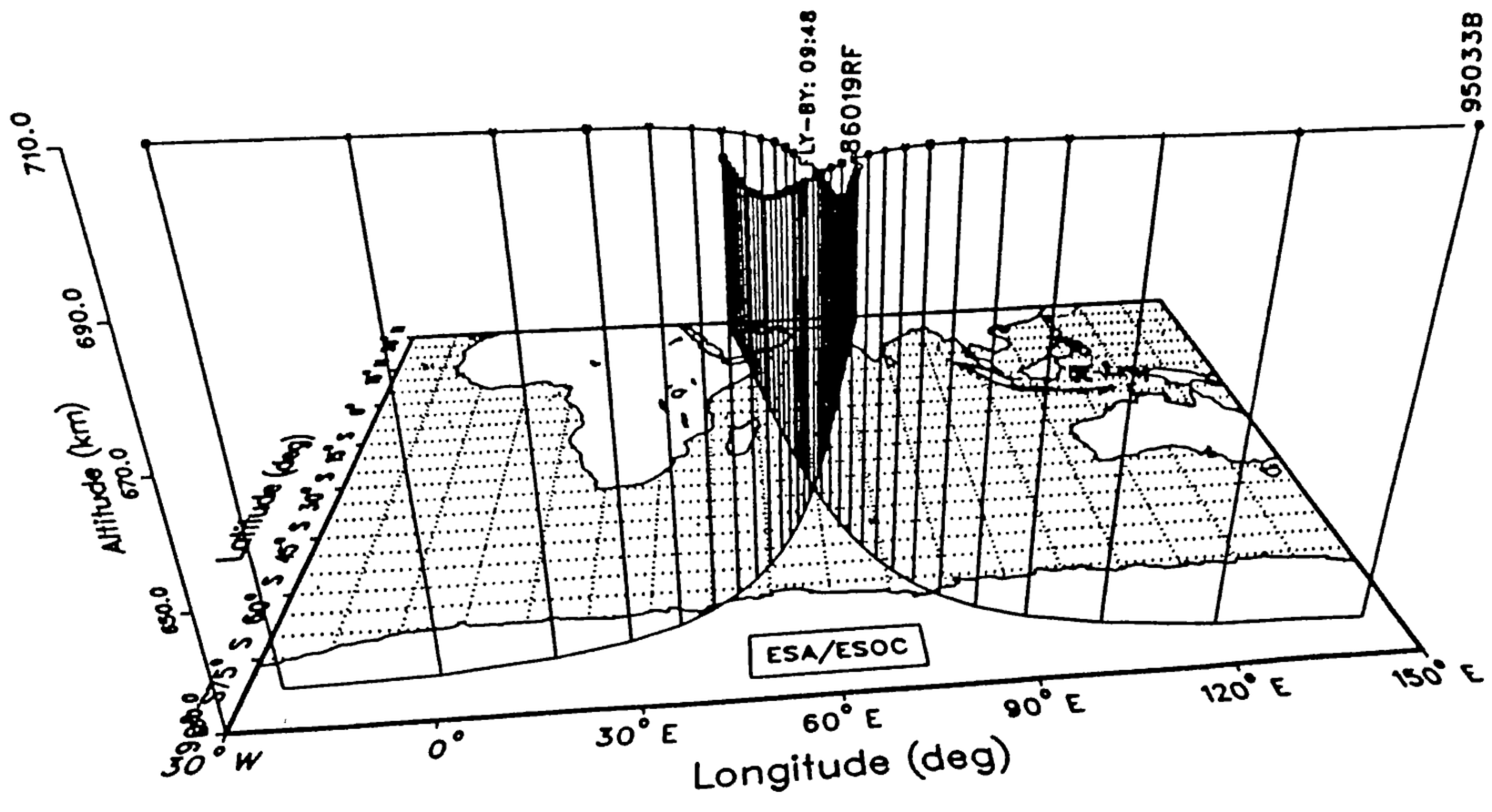

Fig.3: Collision of Cerise (95-033B) with a fragment (86-019RF) of the SPOT-1 launcher upper stage on 24-Jul-1996 09:48:03 UT at $H = 685.86$ km, $\phi = 38.18°$ S and $\lambda = 59.74°$ E. This is the first confirmed collision between two catalog objects. - The COSPAR numbers indicate the start of the satellite tracks. Track markers are spaced at 1 min intervals.

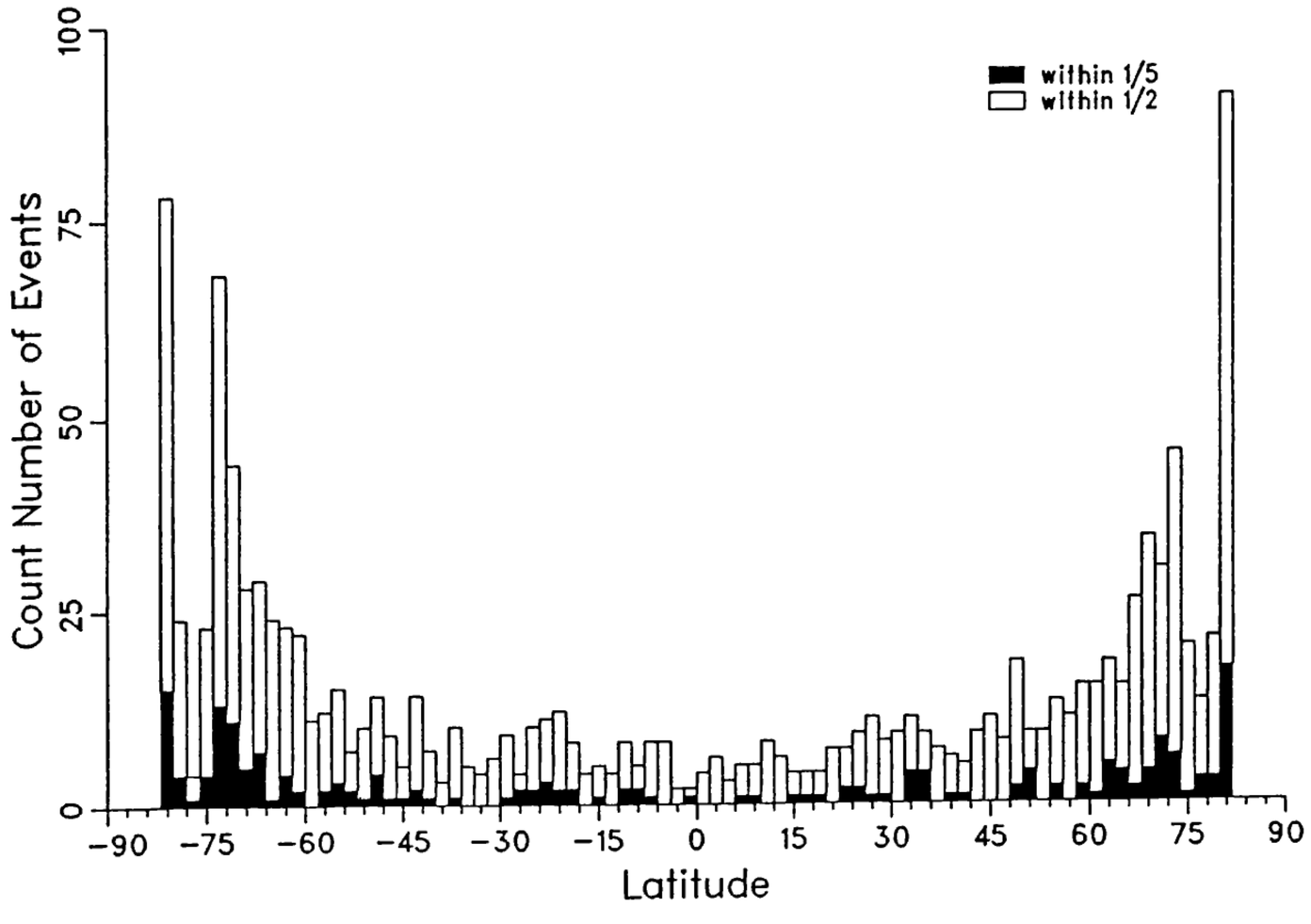

Fig.4: Latitude distribution of combined ERS-1 and ERS-2 conjunction events with catalog objects, for miss distances within 1/2 and 1/5 of the size of the spacecraft centered reference ellipsoid of 25km × 10km × 10km (along-track, radial, out-of-plane). - Analysis time frame: 04-Dec-1995 to 17-Feb-1997.

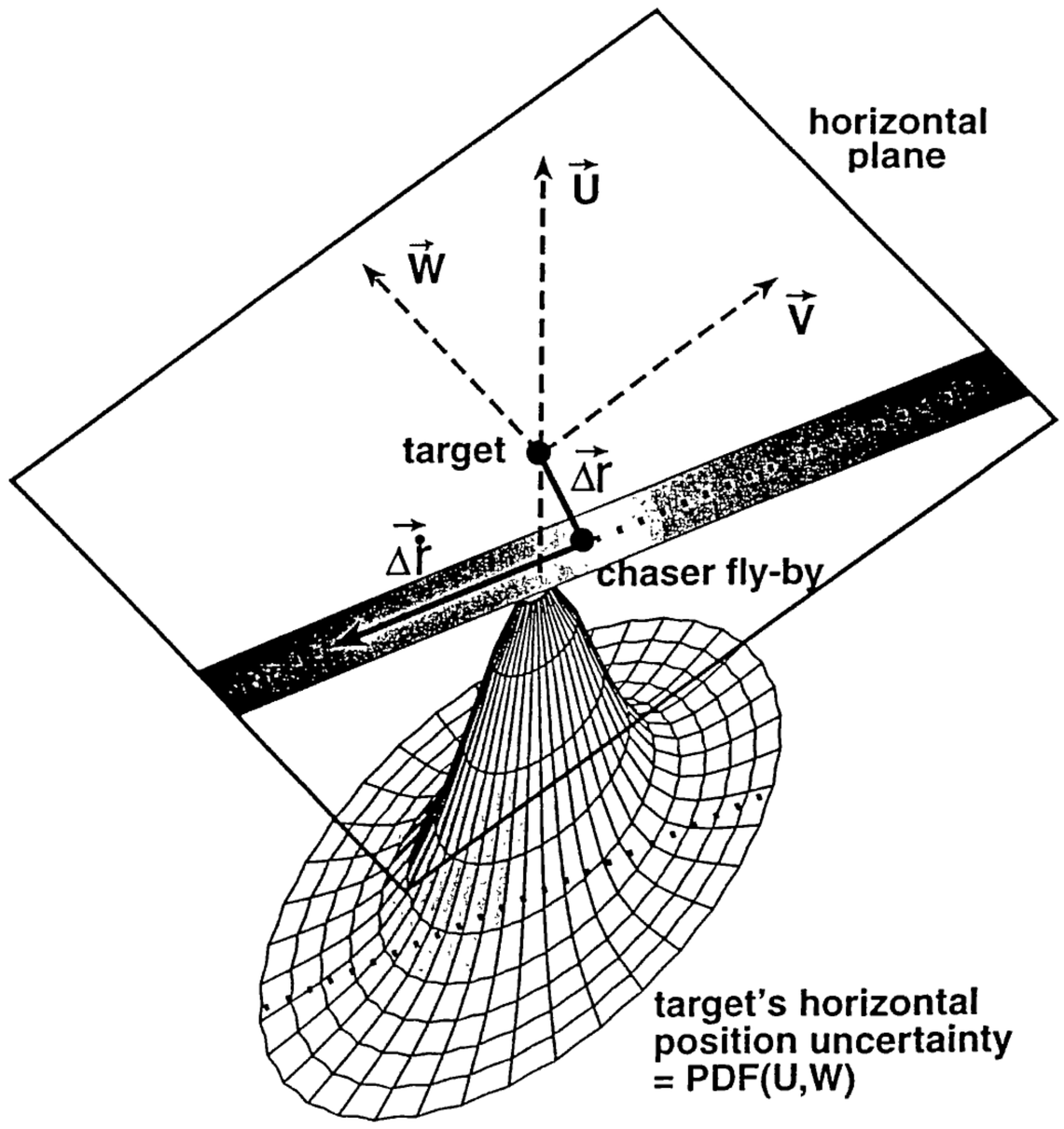

Fig.5: Illustration of the assessment of the collision risk probability for a conjunction event. For simplicity, a planar problem in the local horizontal plane is shown, with a corresponding position probability density function (PDF) of the target. The probability to hit the target along the nominal flight path of the chaser is the integral over the PDF volume swept out by the collision cross-section.

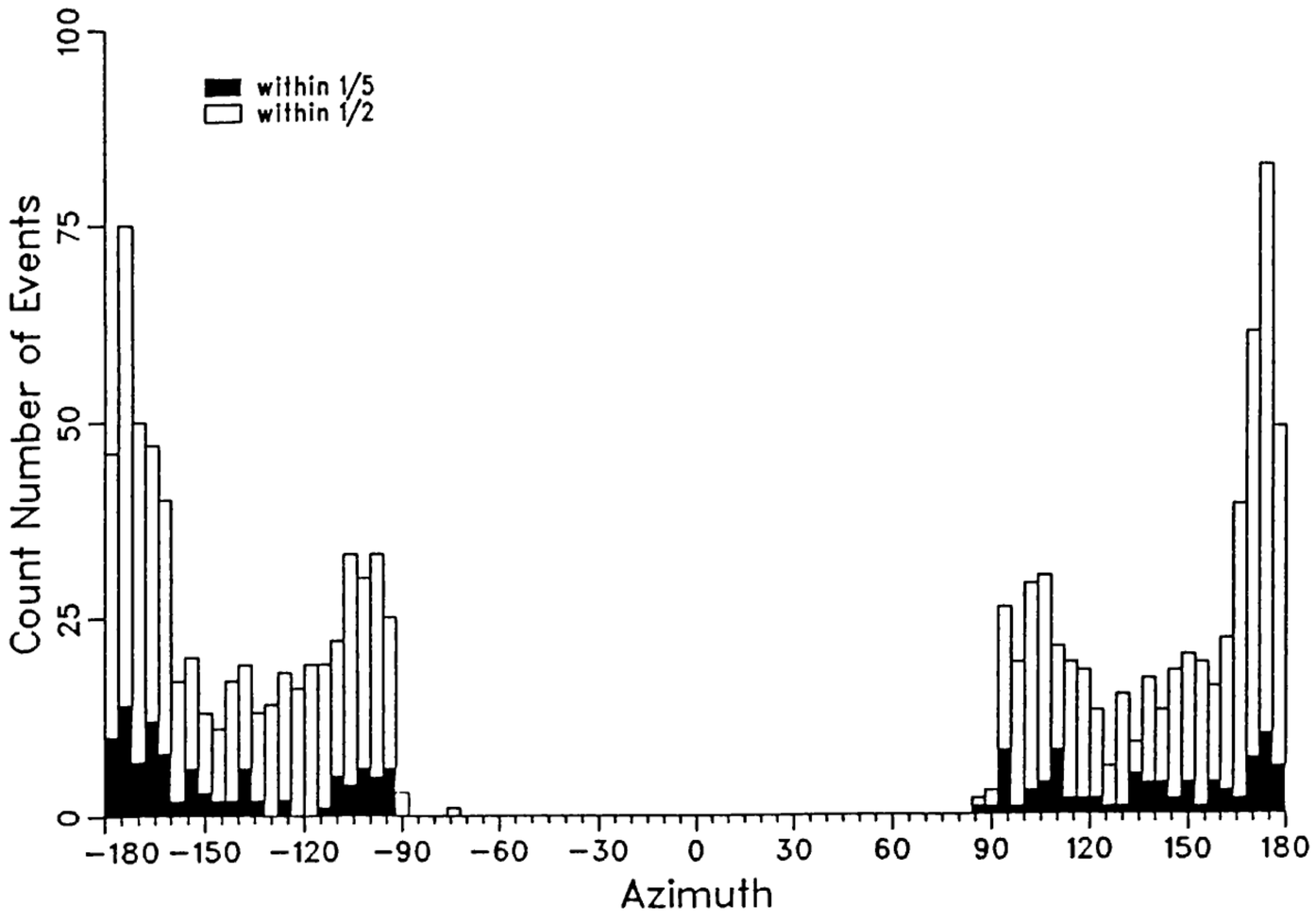

Fig.6: Azimuth distribution of possible impact directions for combined ERS-1 and ERS-2 conjunction events with catalog objects, for miss distances within 1/2 and 1/5 of the size of the spacecraft centered reference ellipsoid of 25km × 10km × 10km (along-track, radial, out-of-plane). - Analysis time frame: 04-Dec-1995 to 17-Feb-1997. Azimuth angles of $A = \pm 180°$ and $\pm 90°$ indicate impacts from the front, and from the side of the spacecraft.

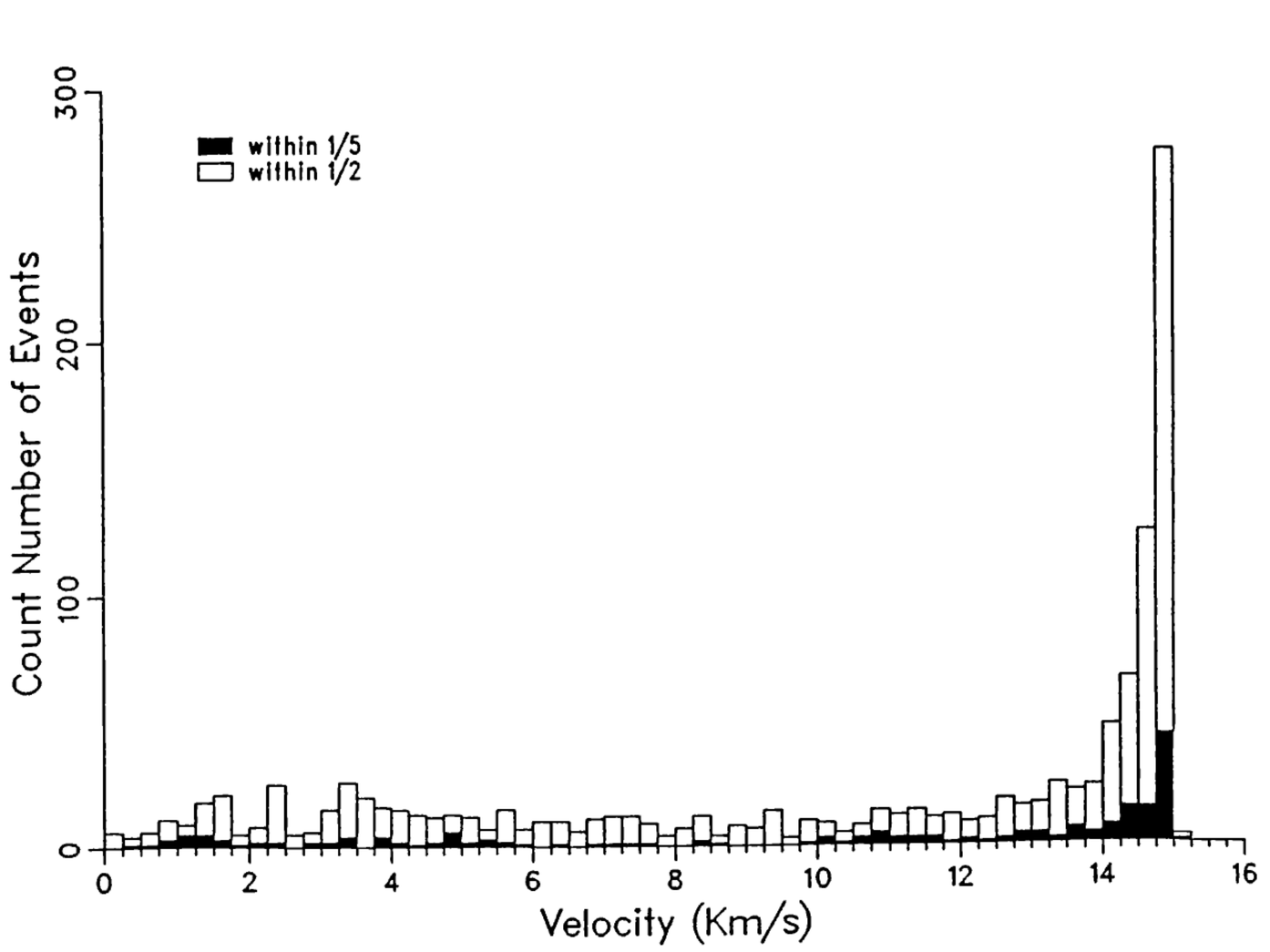

Fig.7: Velocity distribution of possible impacts for combined ERS-1 and ERS-2 conjunction events with catalog objects, for miss distances within 1/2 and 1/5 of the size of the spacecraft centered reference ellipsoid of 25km × 10km × 10km (along-track, radial, out-of-plane). - Analysis time frame: 04-Dec-1995 to 17-Feb-1997. High velocities are associated with impact azimuth directions near $A = \pm 180°$.